(1) Form of the paper

Original Article

(2) Title

Novel transcript profiling of diffuse alveolar damage induced by hyperoxia exposure in

mice: Normalization by glyceraldehyde 3-phosphate dehydrogenase

(3) Authors

Ichiroh Shimada · Kazuhiro Matsui · Bernd Brinkmann · Carsten Hohoff ·

Koichi Hiraga · Yoshiaki Tabuchi · Ichiro Takasaki · Ichiro Kato · Hiroshi Kawaguchi ·

Kumi Takasawa · Reiko Iida · Hisao Takizawa · Takasumi Matsuki

Ichiroh Shimada · Kazuhiro Matsui · Reiko Iida · Takasumi Matsuki

Department of Forensic Medicine, Faculty of Medical Sciences, University of Fukui,

23-3, Matsuokashimoaizuki, eiheiji-cho, Yoshida-gun, Fukui 910-1193, Japan

Bernd Brinkmann · Carsten Hohoff

Institute of Legal Medicine, University of Münster, Röntgenstr. 23, 48149, Münster, Germany

Koichi Hiraga · Ichiro Kato · Hiroshi Kawaguchi · Kumi Takasawa

Department of Biochemistry, Faculty of Medicine, University of Toyama, 2630 Sugitani, Toyama City, Toyama 930-0194, Japan

Yoshiaki Tabuchi · Ichiro Takasaki

Division of Molecular Genetics, Life Scientific Research Center, University of Toyama, 2630 Sugitani, Toyama City, Toyama 930-0194, Japan

Hisao Takizawa

Department of Legal Medicine, Faculty of Medicine, University of Toyama, 2630 Sugitani, Toyama-shi, Toyama 930-0194, Japan

(4) Corresponding Author's address

Takasumi Matsuki

Department of Forensic Medicine,

Faculty of Medical Sciences,

University of Fukui,

23-3, Matsuokashimoaizuki, eiheiji-cho, Yoshida-gun, Fukui 910-1193, Japan

Tel:　+81-776-61-8341

Fax:　+81-776-61-8108

E-mail: ichi@u-fukui.ac.jp (I. Shimada)

Abstract

Under mechanical ventilation with high-inspired oxygen concentration, diffuse alveolar damage (DAD) was found to take place in some patients. To clarify the molecular pathophysiology of this condition we investigated the time course of gene expression changes induced by hyperoxia exposure in mouse lung using real-time quantitative polymerase chain reaction (real-time qPCR). Our results normalized by glyceraldehyde 3-phosphate dehydrogenase showed that mRNA levels of cysteine rich protein 61 (CYR61) and connective tissue growth factor (CTGF) were significantly up-regulated, while those of surfactant-associated protein C (SFTPC), cytochrome P450, 2F2 (CYP2F2), Claudin 1, (CLDN1), membrane-associated zonula occludens protein-1 (ZO-1), lysozyme (LYZS), and P lysozyme structural (LZP-S) were significantly down-regulated. Increasing level of mRNAs, each encoding CYR61 and CTGF, suggests a serious risk of fibrosing alveolitis. Decrease in levels of mRNAs for SFTPC, CYP2F2, CLDN1, ZO-1, LYZS, and LZP-S suggests alveolar dysfunction and disruption of the immune system. Moreover we confirmed apoptotic conditions, such as significant up-regulations of mRNA levels in Myc and Galectin-3. Hyperoxic condition probably yielded reactive oxygen species (ROS), which resulted in a

malignant cycle of ROS production by Myc overexpression.

Introduction

Mechanical ventilation with high-inspired oxygen concentration is often used in care practices for critically ill patients after injury from wound or physical agents. Hyperoxia is a known cause of diffuse alveolar damage (DAD) [1], and it is sometimes identified upon judicial autopsy. For example, we have experienced cases of burn or misuse of respirator equipment, in which DAD was induced due to the association between prolonged use of highly concentrated oxygen and clinical disorders, that is, hypovolemic shock or bacterial pneumonia [2], respectively. We have posited toxic side effects of hyperoxia exposure in medicolegal expert opinions on these cases, however, we have required more objective evidence demonstrating the pathogenesis of DAD. Hyperoxia-exposure induced retinopathy of premature baby [3] has been previously taken into the law court in Japan. Forensically, we should check the toxic side effects of prolonged use of highly concentrated oxygen, in lung, too. We think that to clarify the molecular pathophysiology of hyperoxia-exposure induced lung injury is novel duty of our forensic pathologist as well as anesthesiologist.

Apart from hyperoxia exposure and mechanical ventilation [4], DAD could be caused by various etiology, including paraquat poisoning [5, 6], idiopathic causes [7,

8], and non-thoracic trauma [9].

Histopathologically, DAD is characterized by the influx of protein-rich edema fluid into the air spaces as a consequence of increased permeability of the alveolar-capillary barrier [10]. Type I alveolar cells are easily injured, whereas type II alveolar cells appear to be more resistant in DAD. It is also well known that injury of vascular endothelial cell plays an important role in alveolar damage.

DAD is a disease which has a high mortality rate and leads to fibrosing alveolitis with persistent hypoxemia in serious cases. Improvement in the treatment of patients afflicted with it may have contributed to the recent decline in the mortality rate, however, the future therapeutic approach hopes to diminish inflammation of the alveolar vascular endothelium in the early stage, and to enhance the resolution of pulmonary edema [11].

Mice exposed to 90-95% oxygen concentration die after 4 or 5 days with DAD [12]. Now novel transcript profiling technology including cDNA microarray and real-time qPCR allows the accurate measurement of changes in gene expression [13]. Therefore we examined the time course of gene expression changes using it. To date, no studies have been performed with regard to a comprehensive survey of gene expressions in DAD induced by hyperoxia exposure.

Materials and methods

Animals and hyperoxia exposure

Eight-week-old mice (C57BL/6J, Charles River Japan, Inc.; NINOX Labo Supply Inc., Ishikawa, Japan) were purchased and acclimatized to a 12-h light / 12-h dark cycle starting at 8:00 and 20:00, respectively. Food and water were available ad libitum.

In the first experiment, we carried out cDNA microarray analysis. 8 male mice weighing 22-25g were randomly divided into two groups as follows: 1) 4 mice for control group were bred in atmospheric oxygen; 2) another 4 mice as the hyperoxia exposure group were bred in a metallic chamber for 2 days, into which oxygen, which was supplied from 100% oxygen concentration bomb, flowed at a rate of 0.8 liter / min. The oximeter (COSMOS XO-2000, New Cosmos Electric Co., Ltd, Japan) in the chamber indicated 90-95% oxygen concentration.

In the second and third experiment, we carried out real-time qPCR analysis. 16

male mice weighing 22-25g were randomly divided into 4 groups as follows: 1) 4 mice for control group were bred in atmospheric oxygen; 2) another 12 mice as the hyperoxia exposure group were bred in the metallic chamber for 1 day, 2 days, and 3 days, respectively.

At the end of these experiments, the mice were anesthetized with an intraperitoneal injection of Pentobarbital Sodium (75mg/kg). Heparinized physiological phosphate saline buffer was infused into the left ventricle and blood was bled through the incised right atrium.

These animal experiments were approved by the Toyama Animal Care and Use Committee in University of Toyama (Toyama, Japan).

Histopathological analysis

The lung specimens were fixed in 10 % formaldehyde buffered with PBS (pH 7.2) and then embedded with paraffin. 4 μm tissue sections were prepared for Hematoxylin-Eosin stain or immunohistochemical staining.

The tissue sections were immunostained by the peroxidase method (EnVision System, DAKO Inc., Carpinteria, California) to evaluate the localization and degree of

reactivity for a mouse monoclonal antibody against thyroid transcription factor-1 (TTF-1) (DAKO Inc., California; dilution 1 : 100) [14], nitric oxide synthase 2 (NOS2) (Santa Cruz biotechnology Inc., California; dilution 1 : 500) , matrix metalloproteinase 2 (MMP2) (Santa Cruz biotechnology Inc., California; dilution 1 : 500), and Galectin-3 (Cedarlane Inc., Canada; dilution 1 : 250), respectively. Briefly, after deparaffinization the tissue sections were treated for antigen retrieval with tris buffer solution (TRS) in a wet chamber using microwaves, three times for 5min each [15, 16]. The sections were allowed to cool at room temperature for 30min. The sections were washed in TRS and sequentially treated with 3% H_2O_2 for 15min to exhaust endogenous peroxidase. After washing with TRS and blocking with 5% normal horse serum for 30min, the sections were incubated with a primary antibody in a wet chamber using microwaves for 10min. After three washes with TRS, the peroxidase-labeled polymer from the EnVision System kit was applied for 10min in a wet chamber using microwaves. After washing in TRS, the color was developed with the Vector VIP substrate kit (Vector Laboratories, Burlingame, California), and the tissue sections were counterstained with Mayer's Hematoxylin.

For a negative control, each monoclonal antibody was replaced with normal mouse serum (DAKO Inc., Carpinteria, California).

Measurement of inflammatory cells expressing Galectin-3

The number of alveolar macrophages and other inflammatory cells expressing Galectin-3 was enumerated on 10-randomly chosen visual fields (magnification, ×200) of the tissue sections stained with it. The statistical test of the average number of 10-microscopic fields was performed in SPSS^{TM} (SPSS Japan Inc., Tokyo, Japan).

Separation of total RNA and mRNA

Total RNA was extracted from the lung using an RNeasy Protect Mini Kit (Qiagen Inc., Tokyo, Japan). It should be noted that total RNA samples were treated with RNase-Free DNase (Qiagen Inc., Tokyo, Japan) for 30min at room temperature.

mRNA was extracted from the DNase-treated sample using an GenElute^{TM} mRNA Miniprep Kit (Sigma Inc., Saint Louis, USA) before cDNA microarray analysis was performed.

cDNA microarray analysis

cDNA microarray analysis was performed by IntelliGene^{TM} Mouse CHIP (Code No. X2021, Takara Shuzo Inc., Tokyo, Japan), which were spotted with 4277 cDNA fragments of mouse known genes. cDNA probes were prepared by reverse transcriptase reaction (RT reaction) (Omniscript Reverse Transcriptase, Qiagen Inc., Tokyo, Japan) with Cy3-dUTP (Amersham Pharmacia Biotech Inc., Tokyo, Japan) or Cy5-dUTP (Amersham Pharmacia Biotech Inc., Tokyo, Japan) and mRNA from the lung of both the control and hyperoxia exposure group, respectively, using an RNA Fluorescence Labeling Core Kit (Takara Shuzo Inc., Tokyo, Japan). In the first experiment, the control group was labeled with Cy3 and the hyperoxia exposure group was labeled with Cy5. In the second experiment, the control group was labeled with Cy5 and the hyperoxia exposure group was labeled with Cy3. Identical results were essentially expected. After treatment with RNase H, cDNA probes were purified by gel filtration. Hybridization and washing of the microarray were carried out according to the manufacturer's instructions. In brief, cDNA probe solutions containing both Cy3- and Cy5-labeled cDNA probes were applied to the microarrays, and then the microarrays were covered with a spaced glass cover slip (Takara Shuzo Inc., Tokyo, Japan) and placed in a humidified chamber at 65°C for 16h. Following this, the microarrays were

sequentially washed in 2× SSC (150mM NaCl and 15mM sodium citrate) containing

0.2% SDS for 5min twice at 55˚C, in 2× SSC containing 0.2% SDS for 5min once at

65˚C, and in 0.05× SSC for 1min once at room temperature. The microarrays were

scanned in both Cy3 and Cy5 channels with a ScanArray Lite (Packard BioChip

Technologies, Billerica, MA, USA). QuantArray software (Packard BioChip

Technologies, USA) was used for image analysis. Genes were considered to be

positively-expressed if the signal / background ratio was >3.0. The average of Cy3 and

Cy5 signals for glyceraldehyde 3-phosphate dehydrogenase (GAPDH) (8 spots each)

gave a ratio that was used to balance or normalize the signals.

Pathway analysis

To construct signal transduction pathway of DAD, up- and down- regulated genes

from cDNA microarray analysis were analyzed using ingenuity pathway analysis[TM]

(Ingenuity Systems, Inc., Redwood city, California, USA).

Real-time qPCR assay

RT reaction (Omniscript Reverse Transcriptase, Qiagen Inc., Tokyo, Japan) was carried out with DNase-treated total RNA and an oligo $d(T)_{16}$ primer. Real-time qPCR was performed according to the manufacturer's instructions for SYBR Premix Ex Taq^{TM} (Takara Shuzo Inc., Tokyo, Japan) using the specific primers listed in Table 1. Amplification was performed by one round of pre-denaturation at 95°C for 10sec, step-cycle mode of 40 rounds of denaturation at 95°C for 10sec, annealing and extension at 60°C for 40sec. All reactions were performed in an Mx3000P (Stratagene Inc., La Jolla, USA). Fold change was normalized by the expression level of GAPDH.

Statistical analysis

The means, standard errors of the means (SEMs), and statistical analyses were calculated using SPSS^{TM} (SPSS Japan Inc., Tokyo, Japan) in the present study. The unpaired Student's t-test was performed between the control (n = 10 fields, Figs. 1c, e) and hyperoxia exposure group (n = 10 fields, Figs. 1d, e) in histopathological analysis, conversely done between the control (n = 4 mice, Figs. 2, 3) and hyperoxia exposure group (n = 4 mice, Figs, 2, 3) in real-time qPCR assay. P values less than 0.05 were regarded as significant.

Results

Histopathological findings

Histopathological findings together with Hematoxylin-Eosin stain and immunohistochemical staining with Galectin-3 in each group are shown in Fig. 1. Histopathological findings depended on examination of the sample tissues from each of the lung lobes, and were found to be similar.

Hematoxylin-Eosin stain showed no significant difference between the control and the group of two-days' hyperoxia exposure (Figs. 1a, b). Immunohistochemical staining with TTF-1 antibody highlighted the nucleus of type II alveolar cells and Clara cells. It did not enable us to recognize distinct regenerative hyperplasia of type II alveolar cell. Immunohistochemical stainings with NOS2 and MMP2 showed no marked difference between the control and hyperoxia exposure groups.

However, immunohistochemical staining with Galectin-3 of the hyperoxia exposure group revealed that it was significantly expressed in alveolar macrophages

and other inflammatory cells, compared with the control group (Figs. 1c, d, e).

cDNA microarray analysis

In order to assess expression of the genome-wide genes in DAD induced by hyperoxia exposure, we carried out cDNA microarray analysis of mouse lung.

Genes in which the averaged fold change was above 1.5 were listed in Table 2. These were 5 genes in 4277 genes analyzed, which were cysteine rich protein 61 (CYR61), ferritin light chain 1 (FTL1), connective tissue growth factor (CTGF), gamma actin, cytoplasmic 1 (Actg1), and solute carrier family 3, member 2 (Slc3a2). Whereas the averaged fold changes of 30 genes among those were below 0.67. These were hemoglobin, beta adult major and minor chain (Hbb-b1 and Hbb-b2), surfactant-associated protein C (SFTPC), P lysozyme structural (LZP-S), lysozyme (LYZS), cytochrome P450, 2f2 (CYP2F2), and so on, as listed in Table 3.

This cDNA microarray doesn't include Myc, Galectin-3, Occludin (OCLN), Claudin 1 and 18 (CLDN1 and CLDN18), and membrane-associated zonula occludens protein-1 (ZO-1).

Time course of gene expression changes in real-time qPCR assay

We examined the time course of gene expression changes using real-time qPCR.

Fig. 2 showed the time course of gene expression changes in which the raw data were analyzed between the control and hyperoxia exposure group. GAPDH was significantly up-regulated when hyperoxia exposure was continued. In 3 days' exposure, Myc, Galectin-3, CYR61, CTGF, and FTL1 were significantly up-regulated, while Hbb-b2, SFTPC, CYP2F2, CLDN1, ZO-1, LYZS, and LZP-S were significantly down-regulated.

Fig. 3 showed the time course of gene expression changes in which the data normalized by GAPDH were analyzed between the control and hyperoxia exposure group. Five genes including Myc, Galectin-3, CYR61, CTGF, and FTL1 were significantly up-regulated. Except for Galectin-3 and FTL1, the time courses had unidirectional tendencies. On the contrary, ten genes including Hbb-b1, Hbb-b2, SFTPC, CYP2F2, OCLN, CLDN 1 and 18, ZO-1, LYZS, and LZP-S were significantly down-regulated and mRNA levels decreased more and more when hyperoxia exposure was continued.

Discussion

To clarify the molecular pathophysiology of DAD induced by hyperoxia exposure,

we examined lungs of mice which were bred under high oxygen concentration for 1, 2,

and 3 days. We used GAPDH to normalize the expression levels of the target mRNAs.

The GAPDH was significantly up-regulated when hyperoxia exposure was continued

(Fig. 2). Analysis of raw data (Fig. 2) and analysis of GAPDH-normalized data (Fig. 3)

showed that twelve genes except for Hbb-b1, OCLN, and CLDN18 were similarly up-

or down-regulated in the second and third experiment of 3 days' exposure. The

biological significance of these three genes requires confirmation by future analysis.

We posit that other twelve results normalized by GAPDH have a biological significance

in hyperoxia-induced DAD, because the time courses of expression changes for these

genes had similar tendencies between the second and third experiment.

Histopathologically, Hematoxylin-Eosin stain and immunohistochemical staining

with TTF-1, NOS2, and MMP2 showed no significant difference between the control

and hyperoxia exposure groups.

However, immunohistochemical staining with Galectin-3 of the hyperoxia

- 18 -

exposure group revealed that it was significantly expressed in alveolar macrophage and other inflammatory cells. Moreover, mRNA levels of Galectin-3 and Myc were significantly up-regulated in the hyperoxia exposure group. These imply undergoing apoptosis because Galectin-3 is an anti-apoptotic lectin that protects macrophages or T cells from death triggered by a variety of agents [17], and aberrant expression of Myc induces apoptosis [18].

Additionally, we assessed expression of the other genes which were selected from evidence of cDNA microarray analysis and its pathway analysis or articles on DAD. CYR61, CTGF, and FTL1 were significantly up-regulated, while Hbb-b2, SFTPC, CYP2F2, CLDN1, ZO-1, LYZS, and LZP-S were significantly down-regulated. The time courses of expression changes for these genes had unidirectional tendencies except for Galectin-3 and FTL1.

FTL1 encodes ferritin light chain 1 [19]. The functional molecule made of 24 identical subunits contains a central cavity, into which up to 4,500 insoluble iron ions is deposited. H-rich ferritins (H subunit, molecular weight; 21,000) have been shown to accumulate or release iron faster than L-rich ferritins (L subunit, molecular weight; 19,000). Therefore, a greater proportion of H subunits is observed in erythropoietic tissue, and a greater proportion of L subunits is found in iron-storing tissue such as

liver [20]. Sharkey et al. reported that initial serum ferritin elevation level correlated with the subsequent development of DAD [21]. Our result suggests the hyperfunction of reticulo-endothelial system due to process hemorrhaging which results from increased permeability of the alveolar-capillary barrier.

Hbb-b1 and Hbb-b2 exist in the cluster [22]. β-minor globin (Hbb-b2) gene expression is preferentially reduced in EKLF (erythroid Kruppel-like factor) knock-out mice and expression of the β-minor globin gene is more affected by EKLF deprivation than the β-major gene (Hbb-b1) [23]. This phenomenon is partially consistent with our observations, in which erythroid transcription factors such as EKLF appear to interact with the state of high oxygen concentration.

CYR61 plays essential roles in embryonic vascular development, while CTGF is secreted by vascular endothelial cells and promotes proliferation and differentiation of chondrocytes and enhances fibroblast growth factor-induced DNA synthesis. CTGF is expressed in advanced atherosclerotic lesions [24] or in renal fibrosis induced by hypoxia [25]. Bork proposed to group these genes under the denomination "CCN family" for CTGF, Cef10/CYR61, and nov [26]. The significance of the CCN family is underscored by the finding that targeted disruptions of CCN1 (CYR61) and CCN2 (CTGF) both lead to lethality in mice. Both CCN1 and CCN2 promote a broad

spectrum of cellular processes, including cell adhesion [27], migration, proliferation, and differentiation. Increasing levels of mRNAs each encoding CYR61 and CTGF suggest a serious risk for developing fibrosing alveolitis relevant to the inappropriate wound healing after DAD.

SFTPC encodes pulmonary surfactant-associated protein C (SP-C) [28], which promotes alveolar stability by lowering the surface tension at the air-liquid interface in the peripheral air spaces. Pulmonary surfactant consists of 90 % lipid and 10 % protein including four surfactant-associated protein: two hydrophilic carbohydrate-binding glycoproteins which are surfactant-associated protein A and D, and two small hydrophobic proteins which are surfactant-associated protein B and C. SP-C deficient mice develop a severe pulmonary disorder associated with atypical accumulations of intracellular lipids in type II alveolar cell, and emphysema [29]. Our result posits a serious risk for pulmonary collapse and emphysema.

CYP2F2 encodes the cytochrome P450 2F2; Naphthalene dehydrogenase, which belongs to the cytochromes P450 family and is a group of heme-thiolate monooxygenases [30]. This enzyme is involved in an NADPH-dependent electron transport pathway. It oxidizes a variety of structurally unrelated compounds, including steroids, fatty acids, and xenobiotics. Therefore, it catalyzes the production of a very

potentially toxic intermediate that is associated with necrosis of type II alveolar cells

and Clara cells. A decrease in level of mRNA for CYP2F2 implies a serious risk of

pulmonary collapse because of loss of production for lung surfactants in these cells.

Alveolar-capillary barrier, composed of the alveolar epithelia and capillary

endothelia, creates a selective barrier to water and solute flux between alveolar space

and capillary. Especially, tight junctions regulate paracellular permeability of epithelia

and endothelia. Recent reports have suggested that occludin (OCLN) may dimerize,

forming a binding site for membrane-associated zonula occludens protein-1 (ZO-1),

and ZO-1 connects occludin and claudins (CLDNs) to the cytoskeleton [31, 32]. These

molecular weights are 65kDa (OCLN), 22 kDa (CLDN1), 29 kDa (CLDN 18), and

225 kDa (ZO-1), respectively [33, 34]. Alterations in tight junctions occur the influx

of protein-rich edema fluid into the air spaces. Decrease in levels of mRNAs for

CLDN1 and ZO-1 suggests alveolar dysfunction, resulting from formation of hyaline

membrane and collapsed alveoli.

And lysozymes (LYZS) encodes the lysozyme C, type M (milk);

1,4-beta-N-acetylmuramidase C. Mouse has two lysozyme Cs which are type M (milk)

and type P (intestinal) (LZP-S) [35]. Lysozyme C is capable of hydrolysis of

1,4-beta-linkages between N-acetylmuramic acid and N-acetyl-D-glucosamine

residues in peptidoglycan and between N-acetyl-D-glucosamine residues in chitodextrins. In general, this enzyme is present in cytoplasmic granules of the polymorphonuclear neutrophils and has primarily a bacteriolytic function in tissues and body fluids such as tears and saliva. A decrease in levels of mRNAs for LYZS and LZP-S suggests a serious risk for progression of infection because of disruption of the immune system.

Physiologically, reactive oxygen species (ROS) are produced in the electron transport system of mitochondria or NADPH oxidase system of phagocytes. ROS play a crucial role in DAD induced by hyperoxia exposure and there is growing evidence that ROS induce cytokines [36]. A prior oxidative stress, including interleukin-1, can confer resistance or tolerance to subsequent oxidative stress [37, 38, 39]. Treatment with lisofylline inhibits hyperoxia-induced increase in tumor necrosis factor-alpha, interleukin-1β, and interleukin-6 [40]. It is generally accepted that Myc overexpression can induce the production of ROS in mitochondria, leading to DNA damage and genomic instability such as gene amplification and polyploidy [41]. Our result that Myc was significantly up-regulated means that ROS produced by hyperoxia exposure induce Myc overexpression, and finally a malignant cycle of ROS production starts. ROS cause extreme damage to DNA or other cytoplasmic

components, including the plasma membrane or the mitochondrial outer and inner membrane. It leads to morphologic changes of pulmonary vascular endothelia or alveolar epithelia, causing the influx of protein-rich edema fluid into the air spaces in turn.

In conclusion, the mRNA levels of Myc, Galectin-3, CYR61, CTGF and FTL1 were significantly up-regulated, while those of Hbb-b2, SFTPC, CYP2F2, CLDN1, ZO-1, LYZS, and LZP-S were significantly down-regulated in DAD induced by hyperoxia exposure. Up-regulations of CYR61 and CTGF suggest a serious risk for fibrosing alveolitis. Down-regulations of SFTPC, CYP2F2, CLDN1, ZO-1, LYZS, and LZP-S mean alveolar dysfunction and disruption of the immune system. Overexpression of Myc and Galectin-3 implies the onset of apoptosis. Especially, Myc overexpression means a malignant cycle of ROS production in lung. Our present results regarding changes in gene expressions will provide a novel finding in pathogenesis of DAD and open up new avenues for therapeutic intervention.

References

[1] Ichikado K, Suga M, Gushima Y, Johkoh T, Iyonaga K, Yokoyama T, Honda O,

Shigeto Y, Tomiguchi S, Takahashi M, Itoh H, Ikezoe J, Müller NL, Ando M

(2000) Hyperoxia-induced diffuse alveolar damage in pigs: correlation between

thin-section CT and histopathologic findings. Radiology 216(2):531-538

[2] Zhou Z, Kozlowski J, Schuster DP (2005) Physiologic, biochemical, and imaging

characterization of acute lung injury in mice. Am J Respir Crit Care Med

172:344-351

[3] Wright KW, Sami D, Thompson L, Ramanathan R, Joseph R, Farzavandi S (2006)

A physiologic reduced oxygen protocol decreases the incidence of threshold

retinopathy of prematurity. Trans Am Ophthalmol Soc 104:78-84

[4] Ikegaki J, Mikawa K, Obara H (1993) Effects of surfactant on lung injury induced

by hyperoxia and mechanical ventilation in rabbits. J Anesth 7:66-74

[5] Ishida Y, Takayasu T, Kimura A, Hayashi T, Kakimoto N, Miyashita T, Kondo T

(2006) Gene expression of cytokines and growth factors in the lungs after

paraquat administration in mice. Legal Med 8:102-109

[6] Orito K, Suzuki Y, Matsuda H, Shirai M, Akahori F (2004) Chymase is activated in

the pulmonary inflammation and fibrosis induced by paraquat in hamsters. Tohoku

J Exp Med 203:287-294

[7] Katzenstein AA, Myers JL (1998) Idiopathic pulmonary fibrosis. Am J Respir Crit
Care Med 157:1301-1315

[8] Chilosi M, Poletti V, Zamo A, Lestani M, Montagna L, Piccoli P, Pedron S, Bertaso
M, Scarpa A, Murer B, Cancellieri A, Maestro R, Semenzato G., Doglioni C
(2003) Aberrant Wnt/β-catenin pathway activation in idiopathic pulmonary
fibrosis. Am J Pathol 162:1495-1502

[9] Dechert RE. The pathophysiology of acute respiratory distress syndrome (2003)
Respir Care Clin N Am 9(3):283-296

[10] Ware LB, Matthay MA (2000) The acute respiratory distress syndrome. N Engl J
Med 342(18):1334-1349

[11] Geiser T (2003) Mechanisms of alveolar epithelial repair in acute lung injury - a
translational approach. Swiss Med Wkly 133:586-590

[12] Barazzone C, Horowitz S, Donati YR, Rodriguez I, Piguet P-F (1998) Oxygen
toxicity in mouse lung: pathways to cell death. Am J Respir Cell Mol Biol
19(4):573-581

[13] Tabuchi Y, Kondo T, Suzuki Y, Obinata M (2005) Genes involved in
nonpermissive temperature-induced cell differentiation in Sertoli TTE3 cells

bearing temperature-sensitive simian virus 40 large T-antigen. Biochem Biophys Res Commun 329:947-956

[14] Holzinger A, Dingle S, Bejarano PA, Miller MA, Weaver TE, Dilauro R, Whitsett JA (1996) Monoclonal antibody to thyroid transcription factor-1: production, characterization, and usefulness in tumor diagnosis. Hybridoma 15(1):49-53

[15] Kumada T, Tsuneyama K, Hatta H, Ishizawa S, Takano Y (2004) Improved 1-h rapid immunostaining method using intermittent microwave irradiation: practicability based on 5 years application in Toyama Medical and Pharmaceutical University Hospital. Modern Pathology 17:1141-1149

[16] Tatsu K, Hayashi S, Shimada I, Matsui K (2005) Cyclooxygenase-2 in sporadic colorectal polyps: Immunohistochemical study and its importance in the early stages of colorectal tumorigenesis. Pathology-Research and Practice 201:427-433

[17] Hoyer KK, Pang M, Gui D, Shintaku IP, Kuwabara I, Liu F-T, Said JW, Baum LG, Teitell MA (2004) An anti-apoptotic role for Galectin-3 in diffuse large B-cell lymphomas. Am J Pathol 164(3):893-902

[18] Sears RC, Nevins JR (2002) Signaling networks that link cell proliferation and cell fate. J Biol Chem 277(14):11617-11620

[19] Renaudie F, Boulanger L, Grandchamp B, Beaumont C (1995) Cloning,

characterization and expression of mouse ferritin L subunit gene. C R Acad Sci Ⅲ 318(4):431-437

[20] Beaumont C, Dugast I, Renaudie F, Souroujon M, Grandchamp B (1989) Transcriptional regulation of ferritin H and L subunits in adult erythroid and liver cells from the mouse. J Biol Chem 264(13):7498-7504

[21] Sharkey RA, Donnelly SC, Connelly KG, Robertson CE, Haslett C, Repine JE (1999) Initial serum ferritin levels in patients with multiple trauma and the subsequent development of acute respiratory distress syndrome. Am J Respir Crit Care Med 159(5),1506-1509

[22] Jahn CL, Hutchison CA, Phillips SJ, Weaver S, Haigwood NL, Voliva CF, Edgell MH (1980) DNA sequence organization of the β-globin complex in the BALB/c mouse. Cell 21(1):159-168

[23] Porcu S, Poddie D, Melis M, Cao A, Ristaldi MS (2005) β-minor globin gene expression is preferentially reduced in EKLF knock-out mice. Gene 351:11-17

[24] Oemar BS, Werner A, Garnier J-M, Do D-D, Godoy N, Nauck M, Marz W, Rupp J, Pech M, Luscher TF (1997) Human connective tissue growth factor is expressed in advanced atherosclerotic lesions. Circulation 95:831-839

[25] Higgins DF, Biju MP, Akai Y, Wutz A, Johnson RS, Haase VH (2004) Hypoxic

induction of Ctgf is directly mediated by Hif-1. Am J Physiol Renal Physiol 287:1223-1232

[26] Bork P (1993) The modular architecture of a new family of growth regulators related to connective tissue growth factor. FEBS 327(2):125-130

[27] Chen C-C, Chen N, Lau LF (2001) The angiogenic factors Cyr61 and connective tissue growth factor induce adhesive signaling in primary human skin fibroblasts. J Biol Chem 276(13):10443-10452

[28] Glasser SW, Korfhagen TR, Bruno MD, Dey C, Whitsett JA (1990) Structure and expression of the pulmonary surfactant protein SP-C gene in the mouse. J Biol Chem 265(35):21986-21991

[29] Glasser SW, Detmer EA, Ikegami M, Na C-L, Stahlman MT, Whitsett JA (2003) Pneumonitis and emphysema in sp-C gene targeted mice. J Biol Chem 278(16):14291-14298

[30] Ritter JK, Owens IS, Negishi M, Nagata K, Sheen YY, Gillette JR, Sasame HA (1991) Mouse pulmonary cytochrome P-450 naphthalene hydroxylase: cDNA cloning, sequence, and expression in Saccharomyces cerevisiae. Biochemistry 30(48):11430-11437

[31] Felinski EA, Antonetti DA (2005) Glucocorticoid regulation of endothelial cell tight junction gene expression: novel treatments for diabetic retinopathy. Current Eye Research 30:949-957

[32] Wu S, Lim K-C, Huang J, Saidi RF, Sears CL (1998) Bacteroides fragilis enterotoxin cleaves the zonula adherens protein, E-cadherin. Proc Natl Acad Sci 95:14979-14984

[33] Morita K, Furuse M, Fujimoto K, Tsukita S (1999) Claudin multigene family encoding four-transmembrane domain protein components of tight junction strands. Proc Natl Acad Sci 96:511-516

[34] Willott E, Balda MS, Heintzelman M, Jameson B, Anderson JM (1992) Localization and differential expression of two isoforms of the tight junction protein ZO-1. Am J Physiol 262(5 Pt 1):C1119-C1124

[35] Cross M, Renkawitz R (1990) Repetitive sequence involvement in the duplication and divergence of mouse lysozyme genes. EMBO J 9 (4):1283-1288

[36] Behr J, Maier K, Krombach F, Adelmann-Grill BC (1991) Pathogenetic significance of reactive oxygen species in diffuse fibrosing alveolitis. Am Rev Respir Dis 144(1):146-150

[37] Faust-Chan R, Hybertson B, Flores SC, Wright RM, Repine JE (1999) Initiation

and tolerance to acute lung injury: Yin-Yang mechanisms involving interleukin-1.
Chest 116:102S-103S

[38] Brown JM, White CW, Terada LS, Grosso M, Shanley PF, Mulvin DW, Banerjee
A, Whitman GJR, Harken AH, Repine JE (1990) Interleukin 1 pretreatment
decreases ischemia/reperfusion injury. Proc Natl Acad Sci 87:5026-5030

[39] White CW, Ghezzi P, Dinarello CA, Caldwell SA, McMurtry IF, Repine JE
(1987) Recombinant tumor necrosis factor/cachectin and interleukin 1
pretreatment decreases lung oxidized glutathione accumulation, lung injury, and
mortality in rats exposed to hyperoxia. J Clin Invest 79:1868-1873

[40] George CLS, Fantuzzi G, Bursten S, Leer L, Abraham E (1999) Effects of
lisofylline on hyperoxia-induced lung injury. Am J Physiol Lung 276:776-785

[41] Thompson EB. The many roles of c-Myc in apoptosis (1998) Annu Rev Physiol
60:575-600

Legends to Figures

Fig. 1

Hematoxylin-Eosin stain of the control group (a) and the group of two-days' hyperoxia exposure (b), in the lung tissues from mice. It showed no significant difference between the control and hyperoxia exposure groups.

Immunohistochemical staining with Galectin-3 of the control group (c) and the group of two-days' hyperoxia exposure (d), in the lung tissues from mice. The hyperoxia exposure group revealed that it was significantly expressed in alveolar macrophages and other inflammatory cells, compared with the control group.

The number of cells expressing Galectin-3 is enumerated on 10-randomly chosen visual fields (magnification, $\times 200$) of the tissue sections stained with Galectin-3 (e). Bars show means and error bars show standard errors of the means (SEMs). Unpaired Student's t-test is performed between the control and hyperoxia exposure groups. P value was less than 0.001 (***$p < 0.001$).

Fig. 2

Time course of gene expression changes in DAD induced by hyperoxia exposure.

White and black bars show data of the second and third experiment, respectively. The

raw data are analyzed between the control and hyperoxia exposure group. Each of fold

changes for hyperoxia exposure groups was divided by averages of those for the control

groups. Accordingly, fold change indicates 1.0 if data for both the control and

hyperoxia exposure groups are same. Bars show means and error bars show standard

errors of the means (SEMs). Unpaired Student's t-test is performed between the control

and hyperoxia exposure groups. P values less than 0.05 are regarded as significant:

*$p<0.05$, **$p<0.01$, ***$p<0.001$. mRNA level for GAPDH is significantly up-regulated

when hyperoxia exposure is continued. In 3 days' exposure, Myc, Galectin-3, CYR61,

CTGF, and FTL1 are significantly up-regulated, while Hbb-b2, SFTPC, CYP2F2,

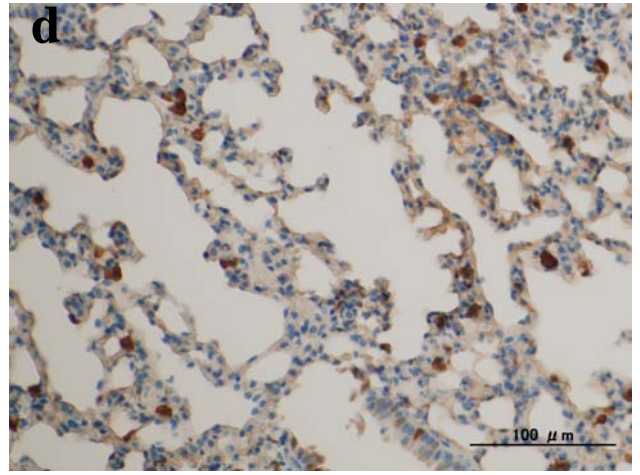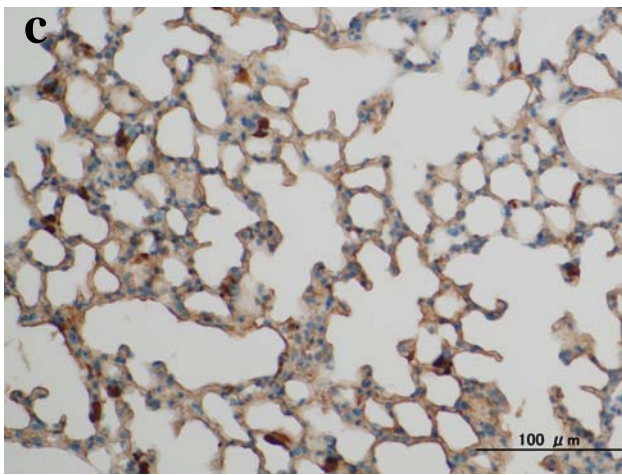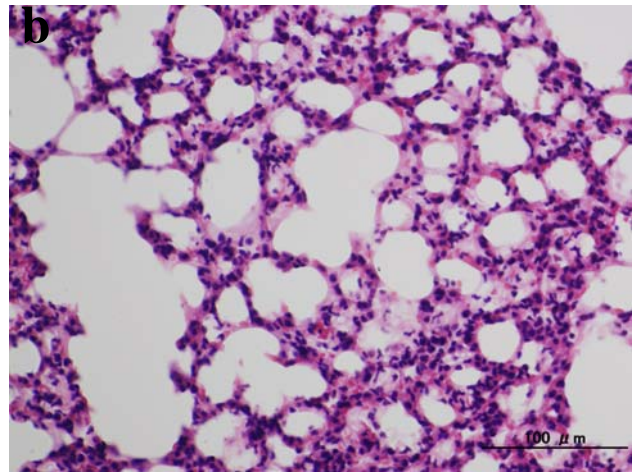CLDN1, ZO-1, LYZS, and LZP-S are significantly down-regulated.

Fig. 3

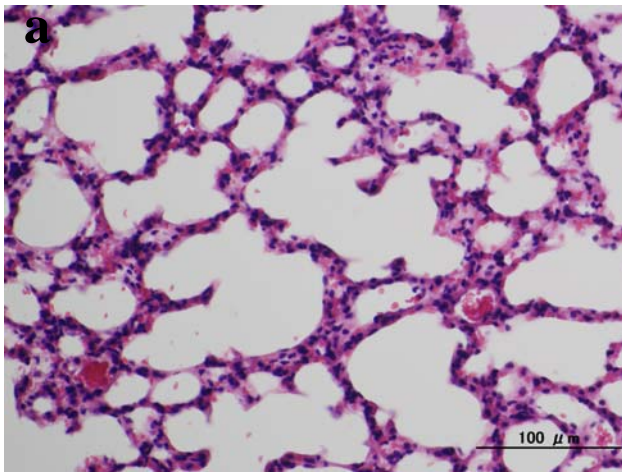   Time course of gene expression changes in DAD induced by hyperoxia exposure.

White and black bars show data of the second and third experiment, respectively, as Fig.

2. The data normalized by GAPDH are analyzed between the control and hyperoxia

exposure groups. mRNA levels for five genes including Myc, Galectin-3, CYR61,

CTGF, and FTL1 are significantly up-regulated. Whereas mRNA levels for ten genes

including Hbb-b1, Hbb-b2, SFTPC, CYP2F2, OCLN, CLDN 1 and 18, ZO-1, LYZS,

and LZP-S are significantly down-regulated.
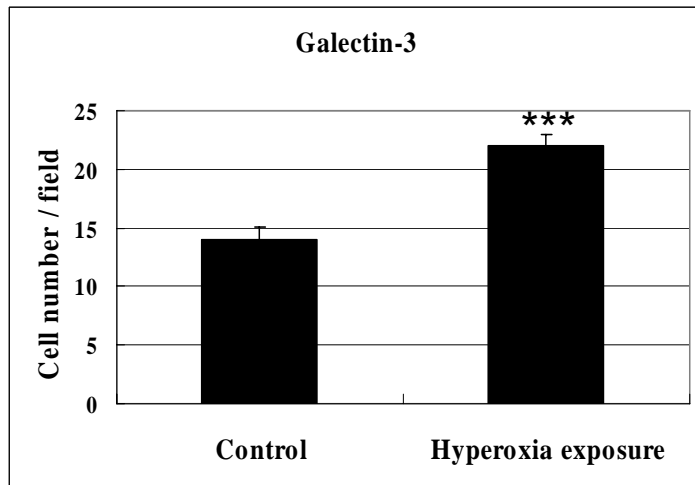
Control　　　　**Hyperoxia exposure**
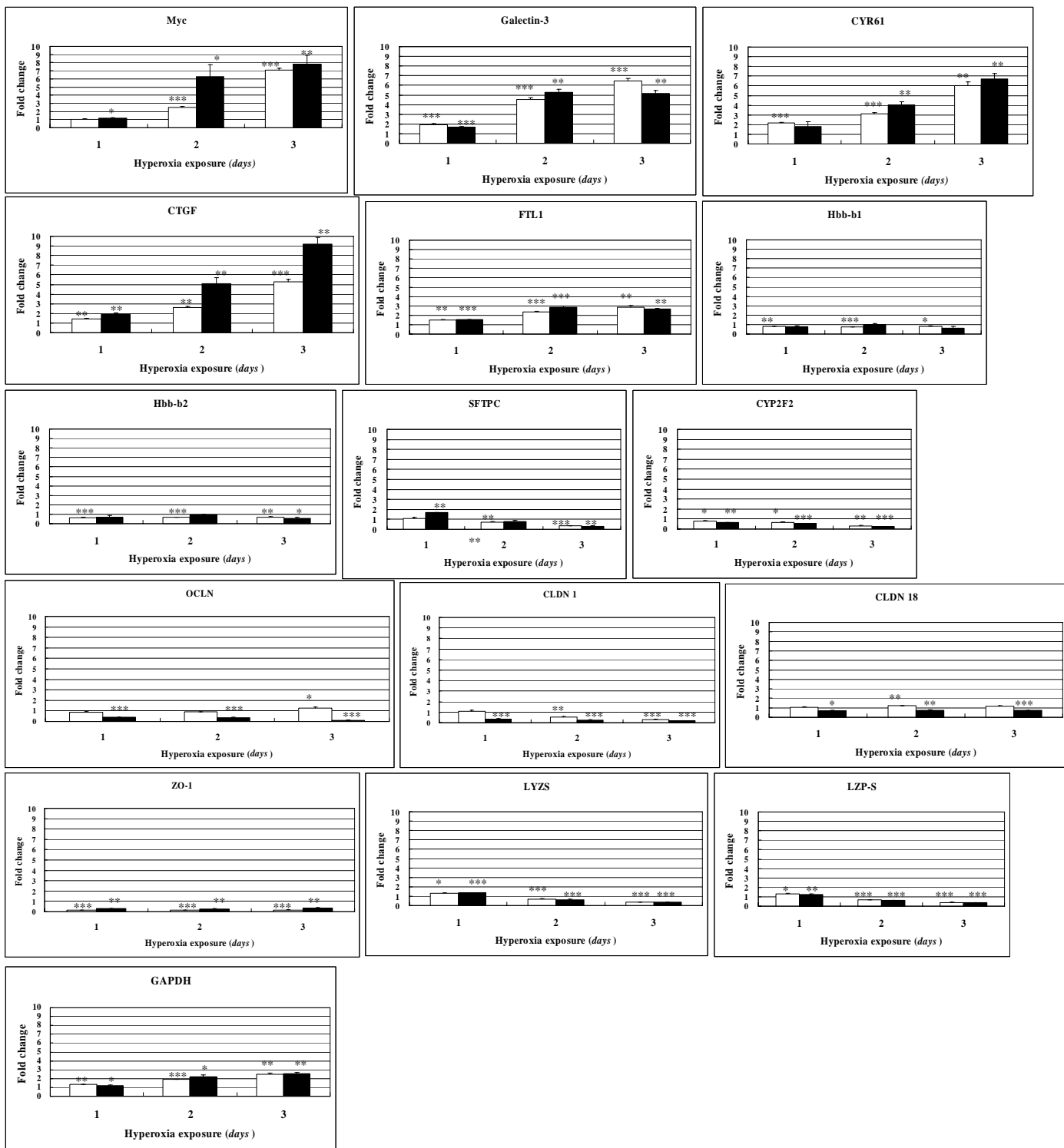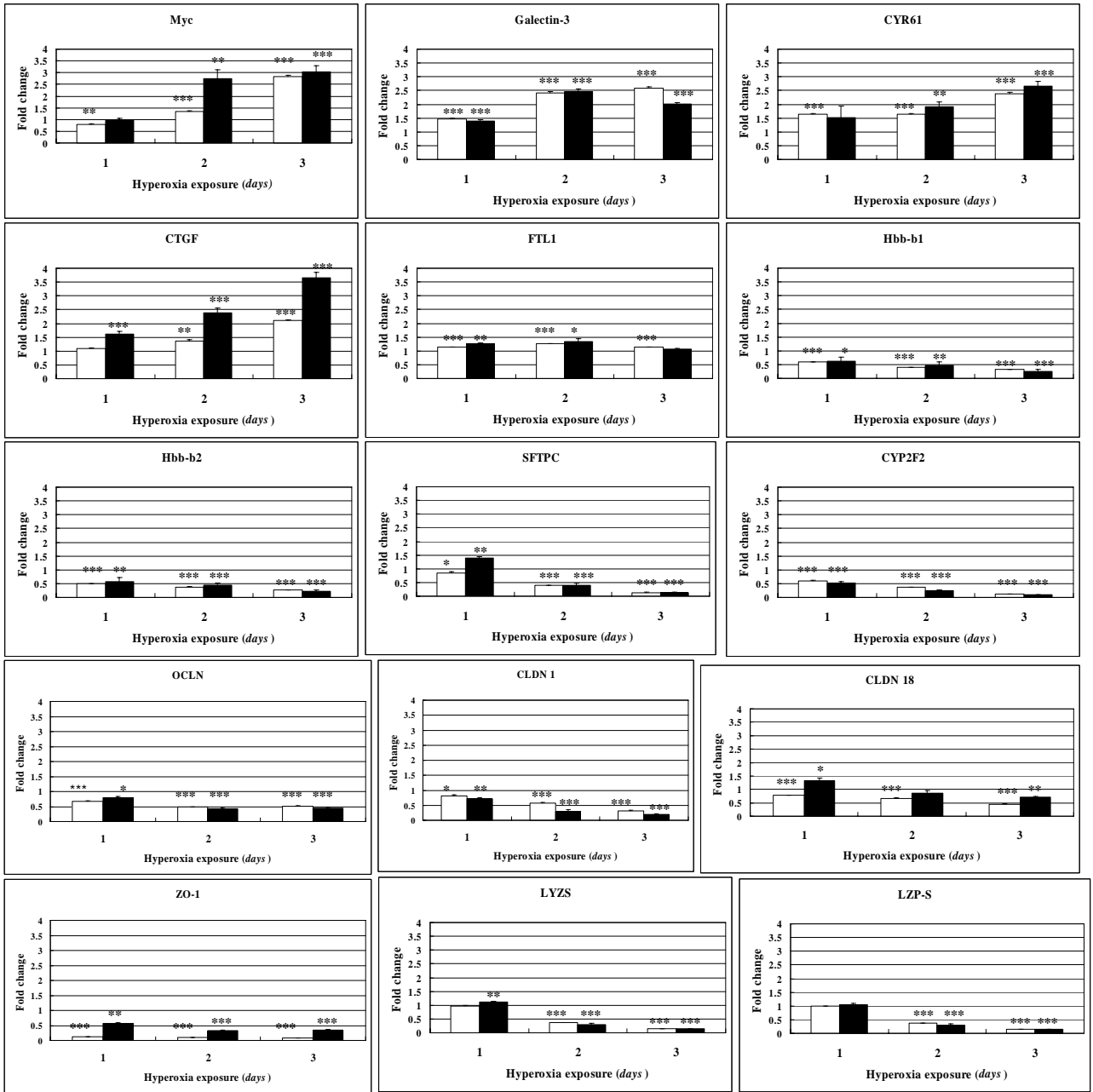

Fig. 1

Fig. 2

Fig. 3

Table 1   Nucleotide sequences of primers for real-time qPCR assay

Gene symbol	GenBank accession no.	Orientation	Nucleotide sequence	Position, Size of the amplified PCR product	
Myc	NM_010849	Sense	5'-GAACTTCACCAACAGGAACTATGAC-3'	596-620	145 bp
		Antisense	5'-GAATTTCTTCCAGATATCCTCACTG-3'	740-716	
Galectin-3	NM_010705	Sense	5'-CAACAGGAGAGTCATTGTGTGTAAC-3'	581-605	118 bp
		Antisense	5'-TTCAACCAGGACTTGTATTTTGAAT-3'	698-674	
CYR61	NM_010516	Sense	5'-AGACCCTGTGAATATAACTCCAGAA-3'	481-505	300 bp
		Antisense	5'-AATTGCGATTAACTCATTGTTTCTC-3'	780-756	
CTGF	NM_010217	Sense	5'-CCAACTATGATGCGAGCCAACTGCC-3'	790-814	356 bp
		Antisense	5'-CCATCGGGGCATTTGAACTCCACTG-3'	1145-1121	
FTL1	NM_010240	Sense	5'-CGAATTGGCCGAGGAGAAGCGCGAG-3'	364-388	393 bp
		Antisense	5'-TAGTCGTGCTTGAGAGTGAGGCGCT-3'	756-732	
Hbb-b1	NM_008220	Sense	5'-GGTACTTTGATAGCTTTGGAGACCT-3'	178-202	102 bp
		Antisense	5'-CATCGTTAAAGGCAGTTATCACTTT-3'	279-255	
Hbb-b2	NM_016956	Sense	5'-ACTTGCAACTTCAGAAACAGACATC-3'	10-34	171 bp
		Antisense	5'-AGGTCTCCAAAGCTATCAAAGTACC-3'	180-156	
SFTPC	NM_011359	Sense	5'-GCTCCAGGAACCTACTGCTACATCA-3'	373-397	163 bp
		Antisense	5'-AAGAATCGGACTCGGAACCAGTATC-3'	535-511	
CYP2F2	NM_007817	Sense	5'-GCTGATGACCACACACAACCTGCTC-3'	925-949	355 bp
		Antisense	5'-CTGAGGCGTCTTGAACTGGTCCGAG-3'	1279-1255	
OCLN	NM_008756	Sense	5'-CTGCAGGAGTATAAGAGCTTACAGG-3'	1494-1518	188 bp
		Antisense	5'-TGCTTGCAGTAATTCCTCTTACTTT-3'	1681-1657	
CLDN1	NM_016674	Sense	5'-CAGTGGAAGATTTACTCCTATGCTG-3'	299-323	300 bp
		Antisense	5'-AATTAAAAATATTATGCCCCCAATG-3'	598-574	
CLDN18	NM_019815	Sense	5'-CAACTTCAAAGCTGTGTCTTACCAT-3'	688-712	115 bp
		Antisense	5'-ATCGTAGATCTTCTTGTTTCTGGTG-3'	802-778	
ZO-1	D14340	Sense	5'-GTTGTGTTCCTTAACCCTGACTCTA-3'	2576-2600	138 bp
		Antisense	5'-TGTGAAGAGATGGTGATTGTTCTTA-3'	2713-2689	
LYZS	NM_017372	Sense	5'-GGAATGGAATGGCTGGCTACTATGG-3'	117-141	284 bp
		Antisense	5'-TGCTCGAATGCCTTGGGGATCTCTC-3'	400-376	
LZP-S	NM_013590	Sense	5'-CAGCATGAGAGCAATTATAACACAC-3'	181-205	278 bp
		Antisense	5'-ATATACTGGGACAGATCTCGGTTTT-3'	458-434	
GAPDH	M32599	Sense	5'-GCCATCAACGACCCCTTCAT-3'	134-153	269 bp
		Antisense	5'-ATGATGACCCGTTTGGCTCC-3'	402-383	

Table 2 Genes up-regulated in mice

Gene name	Gene ontology	GenBank accession no.	Ratio 1	Ratio 2	Mean
cysteine rich protein 61 (Cyr61)	growth factor-binding protein, angiogenesis	NM_010516	4.00	3.46	3.73
ferritin light chain 1 (Ftl1)	iron ion homeostasis	NM_010240	2.66	2.00	2.33
connective tissue growth factor (Ctgf)	fibroblast proliferation, angiogenesis	NM_010217	2.44	1.89	2.16
actin, gamma, cytoplasmic 1 (Actg1)	actin cytoskeleton, sarcomere organization	NM_009609	1.48	2.16	1.82
solute carrier family 3, member 2 (Slc3a2)	cell-surface antigen	NM_008577	1.49	1.75	1.62

Table 3 Genes down-regulated in mice

Gene name	Gene ontology	GenBank accession no.	Ratio 1	Ratio 2	Mean
hemoglobin, beta adult minor chain (Hbb-b2)	oxygen and carbon dioxide transport	NM_016956	0.3	0.38	0.34
hemoglobin, beta adult major chain (Hbb-b1)	oxygen and carbon dioxide transport	NM_008220	0.35	0.33	0.34
surfactant-associated protein C (Sftpc)	alveolar stability	NM_011359	0.41	0.34	0.37
P lysozyme structural (Lzp-s)	cell wall catabolism, bacteriolytic function	NM_013590	0.51	0.25	0.38
lysozyme (Lyzs)	cell wall catabolism, bacteriolytic function	NM_017372	0.49	0.32	0.4
cytochrome P450, 2f2 (Cyp2f2)	oxydization of naphthalene, electron transport	NM_007817	0.46	0.38	0.42
RIKEN cDNA 1810057C19 gene (1810057C19Rik)	Unknown	NM_026433	0.4	0.47	0.43
stearoyl-Coenzyme A desaturase 1 (Scd1)	fatty acid biosynthesis, superoxide metabolism	NM_009127	0.54	0.32	0.43
thioether S-methyltransferase (Inmt)	sulfur and selenium metabolism	NM_009349	0.44	0.48	0.46
RIKEN cDNA 2700055K07 gene (2700055K07Rik)	Unknown	NM_026481	0.56	0.36	0.46
myosin, light polypeptide 4 (Myl4)	structural constituent of muscle, muscle contraction	NM_010858	0.49	0.47	0.48
selenium binding protein 2 (Selenbp2)	selenium and acetaminophen binding	NM_019414	0.48	0.53	0.51
troponin T2, cardiac (Tnnt2)	structural constituent of muscle, muscle contraction	NM_011619	0.52	0.53	0.53
ATPase, Ca^{2+} transporting, cardiac muscle, slow twitch 2 (Atp2a2)	contractile function	NM_009722	0.45	0.61	0.53
haptoglobin (Hp)	hemoglobin binding, acute-phase response	NM_017370	0.47	0.59	0.53
sodium/hydrogen exchanger, isoform 3 regulator 2 (Slc9a3r2)	transepithelial sodium absorption	NM_023055	0.6	0.49	0.54
elongation of very long chain fatty acids -like 1 (Elovl1)	elongation of very long chain fatty acids	NM_019422	0.58	0.51	0.55
DNA segment, Chr 4 (D4Wsu53e)	nucleic acid binding	NM_023665	0.56	0.55	0.55
stearoyl-Coenzyme A desaturase 2 (Scd2)	fatty acid biosynthesis, superoxide metabolism	NM_009128	0.59	0.52	0.55
aquaporin 1 (Aqp1)	water transport, integral to plasma membrane	NM_007472	0.54	0.6	0.57
carbonic anhydrase 3 (Car3)	carbonate dehydratase activity, high concentration in muscle	NM_007606	0.6	0.57	0.59
fatty acid binding protein 4, adipocyte (Fabp4)	fatty acid binding, cholesterol homeostasis	NM_024406	0.64	0.54	0.59
cysteine rich protein 2 (Crip2)	hemopoiesis, positive regulation of cell proliferation	NM_024223	0.65	0.56	0.6
opioid growth factor receptor (Ogfr)	opioid receptor activity, modulation of cell proliferation	NM_031373	0.65	0.56	0.6
thyroid hormone responsive SPOT14 homolog (Rattus) (Thrsp)	lipogenesis	NM_009381	0.65	0.57	0.61
dynein, cytoplasmic, light chain 1 (Dnclc1)	protein inhibitor of neuronal NOS, actin filament organizaion	NM_019682	0.64	0.6	0.62
receptor (calcitonin) activity modifying protein 2 (Ramp2)	G-protein coupled receptor protein signaling pathway	NM_019444	0.65	0.63	0.64
transmembrane protein 59 (Tmem59)	Unknown	NM_029565	0.66	0.63	0.65
forkhead box G1 (Foxg1)	forebrain development, ganglia morphogenesis	NM_008241	0.65	0.66	0.65
RIKEN cDNA 2410005O16 gene (2410005O16Rik)	Unknown	NM_025476	0.66	0.67	0.67